Chemical Equilibria in Glass-Forming Melts: High-Temperature ^{31}P and ^{77}Se NMR of the Phosphorus–Selenium System

Robert Maxwell and Hellmut Eckert*

Contribution from the Department of Chemistry, University of California, Santa Barbara, California 93106

Received August 20, 1993®

Abstract: Molten-state equilibria governing the structure of phosphorus–selenium glasses are studied by high-temperature ^{31}P and ^{77}Se NMR over the temperature range 25 °C ≤ T ≤ 550 °C. The spectra reveal that generally ca. 100 K above the glass transition temperature motional narrowing occurs concomitant with characteristic chemical exchange processes. In the fast exchange limit, the ^{31}P and ^{77}Se chemical shifts reflect the average speciations of phosphorus and selenium atoms, respectively. In melts with low phosphorus contents (≤20 atom % P) the ^{31}P NMR spectra are dominated by the chemical equilibrium $PSe_{3/2} + Se \rightarrow Se{=}PSe_{3/2}$. Detailed composition-dependent analysis of the ^{31}P chemical shifts in the fast-exchange limits reveals that this equilibrium is temperature dependent, with a reaction enthalpy around −5 ± 1 kJ/mol and a reaction entropy of −16 ± 1 J/(mol K). In melts with phosphorus contents ≥40 atom %, a thermal depolymerization process results in the formation of molecular P_4Se_3 and $PSe_{3/2}$ groups at the expense of P–P bonded structures. The spectra are analyzed in terms of temperature-dependent equilibrium constants, characterized by a reaction enthalpy of ca. 51 ± 4 kJ/mol and a reaction entropy of 50 ± 7 J/(mol K), respectively. In glass containing 48 atom % P, the phosphorus speciation is affected by hysteresis, due to the crystallization and incongruent melting of P_4Se_4.

Introduction

Non-oxide chalcogenide glasses based on the sulfides, selenides, and tellurides of the main group III–V elements have gained much interest due to their wide transparency window in the 2–10 μm wavelength region.[1] By varying the composition and thermal history of these materials, their optical and electronic properties can be tailored to cover a wide range of physical properties.[2-4] During the past decade, these potential applications have spurred extensive spectroscopic[5] and theoretical[6] efforts to understand the local structure of these materials, and general structural concepts are now emerging slowly. New conceptual approaches have addressed the question of short range order on the basis of average valences and coordination numbers,[7] while the theoretical framework of rigidity percolation[8] has been applied to explain macroscopic properties of covalent networks.[9] Experimentally, EXAFS and diffraction studies appear to indicate the presence of substantial intermediate range order on the 10–20-Å scale in many covalent glasses.[10] On the other hand, solid-state NMR results have indicated the significance of chemical disorder, i.e. the competition of homopolar and heteropolar bonding as an essential feature of glass formation in these systems.[11]

As one representative within this group of materials, the phosphorus–selenium system has been the subject of considerable interest and controversy for approximately two decades.[12] Most recently, evidence from neutron diffraction and Raman spectroscopy has shown that vitreous P_2Se is an interesting example of a zero-dimensional glass, i.e. a disordered assembly mainly comprised of P_4Se_x molecular units.[13,14] However, the structure of glasses in the selenium-rich domain (≤50 atom % P) is still a point of controversy. While EXAFS and neutron diffraction data suggested that these glasses consist of well-defined P_4Se_3, P_4Se_4, and P_4Se_5 cluster units embedded in a selenium-rich matrix,[15] solid-state NMR studies indicate that such intermediate range order structures are far less abundant than previously believed.[16-18] Using a combination of spin–echo and magic angle spinning NMR techniques, the structure of these glasses has been described quantitatively in terms of the following structural units: Se—Se links, tetrahedral $Se{=}PSe_{3/2}$ groups, trigonal

® Abstract published in *Advance ACS Abstracts*, December 15, 1993.

(1) Taylor, P. C. *Mater. Res. Soc. Bull.* **1987**, 36. Nishii, J.; Morimoto, S.; Inagawa, I.; Iizuka, R.; Yamishita, T.; Yamagashi, T. *J. Noncryst. Solids* **1992**, *140*, 199.

(2) Kastner, M. *J. Noncryst. Solids* **1980**, *35–36*, 807. Adler, D. *J. Noncryst. Solids* **1985**, *73*, 205 and references therein.

(3) Pradel, A.; Ribes, M. *Solid State Ionics* **1986**, *18/19*, 351. Zhang, Zh.; H, Kennedy, J. *Solid State Ionics* **1990**, *38*, 217.

(4) Hilton, A. R.; Jones, C. E.; Brau, M. *Phys. Chem. Glasses* **1966**, *7*, 105. T. Kolomiets, B. T. *Phys. Status Solidi* **1964**, *7*, 359, 713. Borisova, Z. U. *Glassy Semiconductors*; Plenum Press: New York, 1981, and references therein.

(5) Elliott, S. R. *Nature (London)* **1992**, *354*, 445. Armand, P.; Ibanez, A.; Dexpert, H.; Philippot, E. *J. Noncryst. Solids* **1992**, *139*, 137. Mastelaro, V.; Dexpert, H.; Benazzeth, S.; Ollitrault-Fichet, R. *J. Solid State Chem.* **1992**, *96*, 301. Boolchand, P. *Hyperfine Interact.* **1986**, *27*, 3.

(6) Angell, C. A. *J. Noncryst. Solids* **1985**, *73*, 1. Vashishta, P.; Kalia, R. K.; Ebbsjø, I. *J. Noncryst. Solids* **1988**, *106*, 301. Antonio, G. A.; Kalia, R. K.; Vashishta, P. *J. Noncryst. Solids* **1988**, *106*, 305.

(7) Liu, Z.; Taylor, P. C. *Solid State Commun.* **1989**, *70*, 81.

(8) Thorpe, M. F. *J. Noncryst. Solids* **1985**, *76*, 109. Phillips, J. C. *J. Noncryst. Solids* **1979**, *34*, 153.

(9) Tatsumisago, M.; Halfpap, B. L.; Green, J. L.; Lindsay, S. M.; Angell, C. A. *Phys. Rev. Lett.* **1990**, *64*, 1549.

(10) Elliott, S. R. *Nature (London)* **1992**, *354*, 445. Phillips, J. C. *J. Noncryst. Solids* **1981**, *43*, 37.

(11) Eckert, H. *Prog. NMR Spectrosc.* **1992**, *24*, 159. Eckert, H. *Angew. Chem. Adv. Mater.* **1989**, *101*, 1763.

(12) Blachnik, R.; Hoppe, A. *J. Noncryst. Solids* **1979**, *34*, 191. *Z. Anorg. Allg. Chem.* **1979**, *457*, 91. Borisova, Z. U. In *Glassy Semiconductors*; Plenum Press: New York, 1981; p 70. Borisova, Z. U.; Kasatkin, B. E.; Kim, E. I. *Izv. Akad. Nauk SSSR, Neorg. Mater.* **1973**, *9*, 822. Kim, E. I.; Chernov, A. P.; Dembovskii, S. A.; Borisova, Z. U. *Izv. Akad. Nauk SSSR, Neorg. Mater.* **1976**, *12*, 1021. Monteil, Y.; Vincent, H. *Can. J. Chem.* **1974**, *52*, 2190; *J. Inorg. Nucl. Chem.* **1975**, *37*, 2053; *Z. Anorg. Allg. Chem.* **1977**, *428*, 259. Heyder, F.; Linke, D. *Z. Chem.* **1973**, *13*, 480. Lathrop, D.; Eckert, H. *J. Am. Chem. Soc.* **1989**, *111*, 3534.

(13) Verrall, D. J.; Elliott, S. R. *J. Noncryst. Solids* **1989**, *114*, 34. Verall, D. J.; Elliott, S. R. *J. Noncryst. Solids* **1988**, *106*, 47.

(14) Phillips, T. R.; Wolverson, D.; Burdis, M. S.; Fang, Y. *Phys. Rev. Lett.* **1989**, *63*, 2574. Rollo, J. R.; Burns, G. R. *J. Noncryst. Solids* **1991**, *127*, 242.

(15) Price, D. L.; Misawa, M.; Susman, S.; Morrison, T. I.; Shenoy, G. K.; Grimsditch, M. *J. Noncryst. Solids* **1984**, *66*, 443. Arai, M.; Johnson, R. W.; Price, D. L.; Susman, S.; Gay, M.; Enderby, J. E. *J. Noncryst. Solids* **1986**, *83*, 80.

(16) Lathrop, D.; Eckert, H. *J. Phys. Chem.* **1989**, *93*, 7895.

(17) Lathrop, D.; Eckert, H. *J. Am. Chem. Soc.* **1990**, *112*, 9017.

(18) Lathrop, D.; Eckert, H. *Phys. Rev. B* **1991**, *43*, 7279.

0002-7863/94/1516-0682$04.50/0

Table 1. Selenium Speciation from ^{77}Se Variable-Temperature NMR Compared to Predictions According to Different Distribution Models[a]

sample	T_g (°C)	α (ppm)	β (ppm/°C)	Se_p:Se_{Se} VT	isolated	cluster	SEDOR
Se	40.0	1318	0.22	0:100	0:100	0:100	
5 atom % P	56.0	1265	0.26	21:79	18:82	10:90	12:88
13 atom % P	76.0	1240	0.20	37:63	47:53	26:74	33:67
20 atom % P	81.4	1188	0.20	60:40	80:20	43:57	48:52
32 atom % P	91.0	1151	0.15	80:20	not possible	70:30	
40 atom % P	94.6	1115	0.18	100:0	not possible	100:0	
P_4Se_3	246.0[b]	1288	0.11				

[a] Coefficients α and β describe the temperature dependence of the ^{77}Se chemical shifts in the fast-exchange limit for selected P–Se glasses. Selenium speciation from ^{77}Se variable-temperature NMR compared to predictions according to different distribution models (see text). Previous results from SEDOR-NMR are included. [b] Melting point.

$PSe_{3/2}$ groups, and $Se_{2/2}P$—$PSe_{2/2}$ units containing a phosphorus–phosphorus bond.[18]

It is important to realize that all of the above structural findings, obtained on melt-quenched glasses, reflect molten-state chemical equilibria that are frozen in at the glass-transition temperature, T_g. To further understand these speciations, and to predict the influence of quenching rates on glass structures, it is important to characterize these equilibria and the thermodynamic parameters involved. In situ high-temperature NMR has proven particularly powerful for this objective, as previously demonstrated by pioneering applications to silicate[19] and phosphorus–sulfur[20] melts. We have also recently published a survey of the chief temperature-dependent features of ^{31}P NMR in the phosphorus–selenium system.[21] The goal of the present contribution is to demonstrate that detailed chemical shift measurements as a function of composition and temperature result in a plethora of structural and thermodynamic information about this system, yielding concentrations for the various types of phosphorus and selenium sites, equilibrium constants describing their interchange in the molten state, and reaction enthalpies and entropies characterizing the temperature dependence of these equilibria.

Experimental Section

Sample Preparation and Characterization. Phosphorus–Selenium glasses containing 5, 13, 20, 30, 32, 35, 40, 45, and 48 atom % P were prepared from the elements as purchased from Aldrich Inc. (P, 99.9%; Se, 99.9%) within evacuated quartz ampules that were heated above 650 °C for at least 48 h, agitated by shaking after 24 h, and cooled slowly in the furnace or quenched rapidly in ice water. Glass transition temperatures were measured on a Dupont 912 dual sample differential scanning calorimeter, using heating rates or 5–10 °C/min, and are listed in Table 1. All of the glasses studied exhibit single T_g's in good agreement with literature data. Low P content glasses show no sign of recrystallization under DSC conditions, while glasses near 50 atom % P recrystallize, forming P_4Se_4, which subsequently melts incongruently. Formation of completely amorphous samples was further verified by X-ray powder diffraction, using a Scintag diffractometer. Crystalline α-P_4Se_3 was obtained by slow cooling of a melt containing a stoichiometric ratio of P and Se and subsequent recrystallization of the product from anhydrous carbon disulfide (HPLC grade). The identity and purity of the product was verified by differential scanning calorimetry, X-ray powder diffraction, and liquid-state NMR in good agreement with literature data. All sample manipulations were carried out in a Vacuum Atmospheres glovebox under anhydrous Ar atmosphere.

NMR Studies. Variable-temperature (VT) NMR spectra were obtained at 121.66 and 81.01 MHz (^{31}P) and at 57.36 MHz (^{77}Se), using General Electric GN-300 and modified Bruker CXP-200 spectrometers equipped with a double-resonance VT static probe manufactured by Doty Scientific. Temperatures were allowed to equilibrate for ca. 30 min, and no appreciable temperature hysteresis effects were noticed. Temperature calibration experiments using the phase transitions in crystalline P_4Se_3 showed that nominal and actual temperatures were within 5 °C, and thus no temperature corrections were applied to the data. Temperature gradient effects were judged to be insignificant by comparing the ^{31}P NMR spectra of crystalline and amorphous samples confined to a variety of sample sizes from a few millimeters to a couple of centimeters in length and 3–5 mm in diameter. Field inhomogeneity contributions to line widths were estimated to be ~20 Hz at room temperature and ~100–200 Hz at 500 °C. Single-pulse ^{31}P NMR spectra were generally recorded with $\pi/4$ pulses of 4-μs length and ^{77}Se spectra with $\pi/2$ pulses of 6.5-μs length to ensure quantitative results over the spectral window of interest. Recycle delays for both ^{31}P and ^{77}Se ranged from a few minutes at $T <$ 200 °C to less than 100 ms at $T >$ 400 °C and were estimated by saturation or inversion recovery experiments.

Results, Data Analysis, and Interpretation

^{77}Se NMR Spectra and Assignments. Parts a–c in Figure 1 show the variable-temperature ^{77}Se NMR spectra of melts containing 5, 20, and 40 mol % P. At temperatures below 200 °C, distinct resonances are observed near 1350 and 1120 ppm, respectively. Based on the influence of composition on the peak ratios (comparison between parts a–c of Figure 1), we assign the 1350-ppm peak to selenium atoms bonded entirely to other Se atoms, whereas the resonance around 1120 ppm is assigned to phosphorus-bonded selenium atoms. In addition, the spectra of the glass containing 40 atom % P also show a hint of molecular P_4Se_3 (peak around 1300 ppm).

As the temperature is increased to ca. 100 K above the glass-transition temperature, the P-bonded and non-P-bonded selenium atoms undergo chemical exchange on the NMR time scale, resulting in characteristic line broadening and coalescence phenomena. The detailed analysis of these characteristic spectra in terms of melt dynamics goes beyond the focus of the present study and will be reported elsewhere.[22] Figure 2 summarizes the temperature dependence of the chemical shifts past the coalescence points, including data for molten selenium. For all of these samples, including pure selenium and P_4Se_3, the chemical shifts become more positive with increasing temperature, with temperature coefficients around 0.2 ppm/K. Linear least-squares fits for the data in Figure 2 are included in Table 1. In the fast exchange region the chemical shifts measured for these samples depend on composition in a straightforward manner, simply reflecting the ratio of Se-only-bonded Se atoms to P-bonded Se atoms. We can estimate these quantitative selenium speciations for each glass by comparison with the chemical shift curves for molten selenium (Se-bonded Se only) and for the melt containing 40 atom % P (P-bonded selenium only). In the latter case, a small correction (10 ppm) has been applied to account for the small P_4Se_3 content of this melt (at 400 °C ca. 7% of the Se is present in this form). Using the experimental data available, the following calibration curves are obtained:

$$\text{Se-only-bonded Se:} \quad \delta/\text{ppm} = 1314 + 0.23T \quad (1a)$$

$$\text{P-bonded Se:} \quad \delta/\text{ppm} = 1105 + 0.18T \quad (1b)$$

where T is given in units of °C. The chemical shift temperature coefficients for these samples are assumed to be intrinsic and not to reflect any chemical changes over the temperature range investigated.

(19) Stebbins, J. F. *Science* **1989**, *245*, 257. Farnan, I.; Stebbins, J. F. *J. Am. Chem. Soc.* **1990**, *112*, 32.
(20) Bjorholm, T.; Jakobsen, H. *J. Am. Chem. Soc.* **1991**, *113*, 27.
(21) Maxwell, R.; Eckert, H. *J. Am. Chem. Soc.* **1993**, *115*, 4747.
(22) Maxwell, R.; Eckert, H., to be submitted for publication.

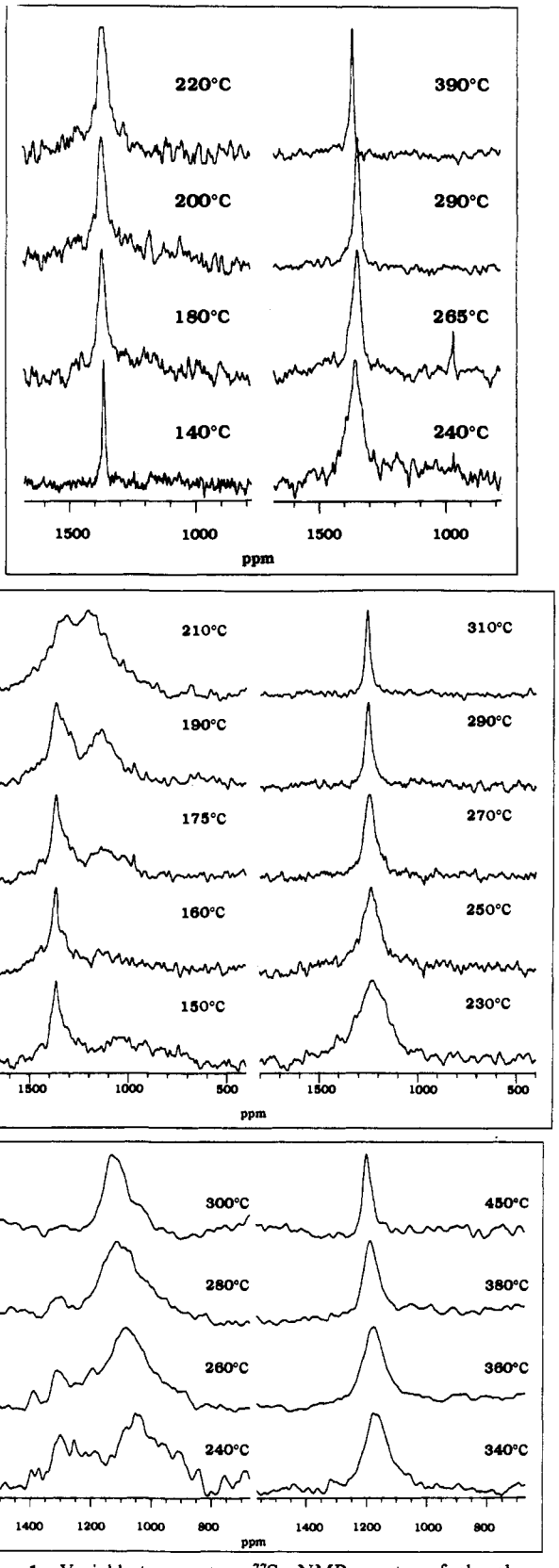

Figure 1. Variable-temperature ^{77}Se NMR spectra of phosphorus–selenium melts: (a, top) 5 atom % P; (b, middle) 20 atom % P; (c, bottom) 40 atom % P.

By interpolation, the data in Table 1 can be used to determine the fractions of P-bonded and Se-only-bonded Se atoms at any temperature. Of particular interest are the speciations obtained at the respective glass-transition temperatures (see Table 1). These data are compared with two extreme predictions: (a) In the "isolated model" all of the P-bonded Se atoms are bonded to one

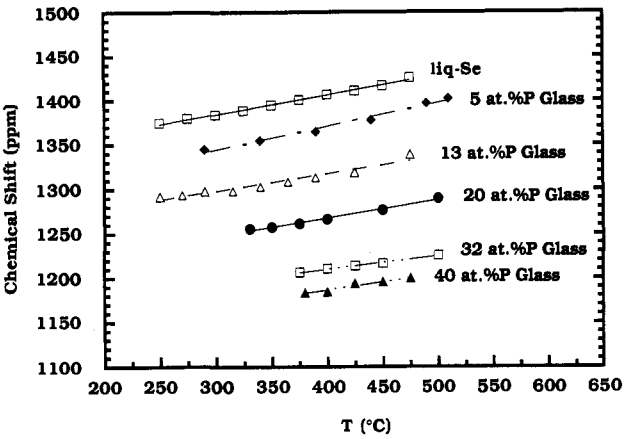

Figure 2. Temperature dependence of the ^{77}Se chemical shifts in phosphorus–selenium melts in the fast-exchange limit.

phosphorus atom only, i.e. they are of the type *Se*═P or Se—*Se*—P. The implication of this model is that the P atoms are isolated from each other and not bridged by selenium. The model also explicitly accounts for the terminal Se atoms that are part of Se═$PSe_{3/2}$ groups, whose concentration is known from MAS-NMR.[16,18] (b) In the "cluster model" it is assumed that all of the P-bonded Se atoms (except for the known number of *Se*═P species) are bridging between two phosphorus atoms.

At low P contents the experimental data are clearly found to be more consistent with the isolated model, whereas at higher P contents the data indicate substantial P–Se–P bridging. Such behavior is entirely expected on the basis of probability arguments. We note that while the actual fractions of P-bonded Se atoms differ somewhat from those determined previously by ^{31}P–^{77}Se spin–echo double resonance (SEDOR) NMR,[17] the trend as a function of P concentration is the same in both studies. Given the assumptions made in the present analysis and the intrinsic limitations of the SEDOR experiment, the agreement can still be considered satisfactory. The most probable systematic error in the SEDOR experiments arises from 180° pulse imperfections on the ^{31}P decoupler channel, resulting in a net underestimation of the number of P-bonded Se atoms. On the other hand, the high-temperature chemical shift analysis presented here is also rather crude, as it assumes that the ^{77}Se chemical shifts of the P-bonded Se atoms are independent of composition. One implication is that, in the absence of information to the contrary, eq 1b is assumed to be valid for all types of P-bonded Se atoms, i.e. *Se*═P, P—*Se*—Se, and P—*Se*—P units.

Table 1 reveals that the temperature coefficient for the melt containing 5 atom % P is slightly higher than that for the other compositions. We believe that this behavior is due to a temperature-dependent speciation equilibrium as is also evident from ^{31}P NMR (see below).

^{31}P NMR Spectra. Parts a–f of Figure 3 show the ^{31}P NMR spectra of P–Se glasses containing 5, 13, 20, 32, 40, and 48 atom % P over their entire respective temperature ranges studied. At and below their glass-transition temperatures, the spectra are dominated by broadening due to wide distributions and large anisotropies of chemical shifts and display resolution no better than previous wideline or MAS NMR spectra. However, at temperatures ca. 100 K above T_g, the liquid eventually attains a viscosity consistent with motional narrowing and averaging by chemical exchange, resulting in resolved ^{31}P resonances. The line shapes seen for these glasses in the 200–300 °C temperature region appear rather complex. As will be discussed elsewhere in detail,[22] the features of these spectra can be simulated satisfactorily if we assume a wide uniform distribution of chemical exchange rates. A consequence of this description is that within a certain temperature range the spectra are superpositions of components in the slow-exchange limit and components showing the effects

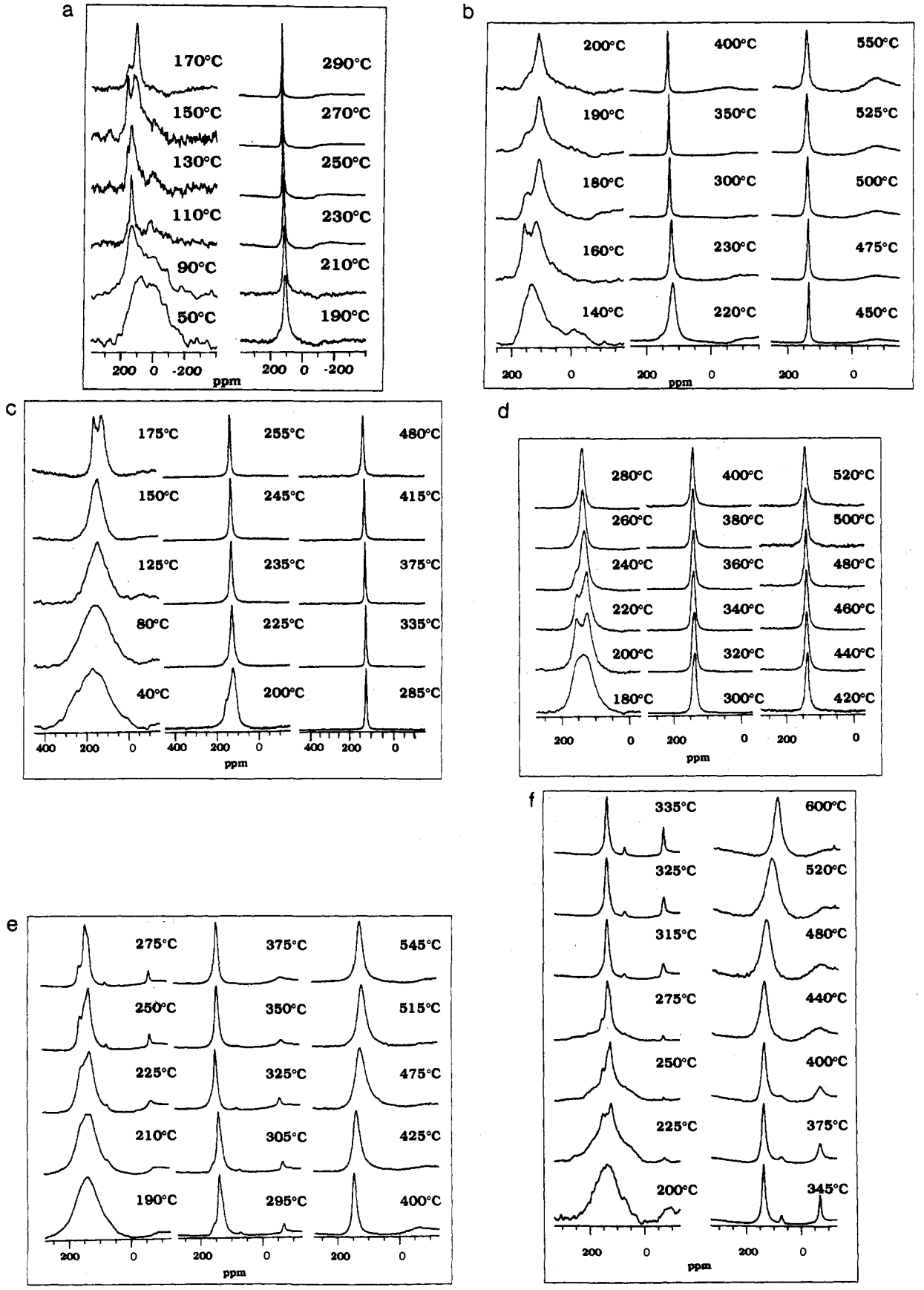

Figure 3. Variable-temperature ^{31}P NMR spectra of phosphorus–selenium melts: (a) 5 atom % P; (b) 13 atom % P; (c) 20 atom % P; (d) 32 atom % P; (e) 45 atom % P; and (f) 48 atom % P.

of exchange averaging. Based on this hypothesis, on comparison with spectra of model compounds, and on our previous MAS NMR studies of these glasses,[18] we arrive at the following peak assignments: At low temperatures, the ^{31}P NMR spectra of the glasses containing 5, 13, and to a lesser extent, 20 atom % P show a discernible shoulder near 0 ppm, which is attributed to four-coordinated $Se{=}PSe_{3/2}$ groups previously identified by room-temperature MAS- NMR studies.[16] As the temperature in-

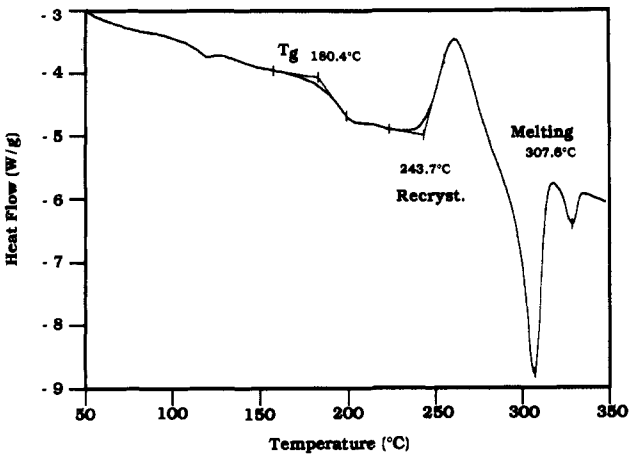

Figure 4. DSC of a glass containing 48 atom % P.

creases, motional narrowing produces a sharp resonance around 153 ppm, which is most consistently assigned to $PSe_{3/2}$ units. In addition, a broader peak appears in the vicinity of 100–120 ppm. The position and shape of this latter peak are strongly composition and temperature dependent, suggesting that this feature arises from chemical exchange between $Se{=}PSe_{3/2}$ (0 ppm) and $PSe_{3/2}$ (153 ppm) groups. Indeed, beyond the point of coalescence the position of this latter peak is fairly consistent with the $Se{=}PSe_{3/2}/PSe_{3/2}$ ratio previously determined by MAS NMR,[18] thus strongly supporting this interpretation.

For glasses with P contents above 32 atom %, the fraction of four-coordinate P atoms is relatively small so that their influence on the spectra is diminished. For these glasses the spectra above 200 °C are dominated by the resonances of $PSe_{3/2}$ groups near 153 ppm and those of P–P bonded structures around 123 ppm, and by the effects of exchange among these sites as the temperature is increased. Finally, glasses with phosphorus contents ≥40 atom % show additional resonances around 70 and −70 ppm, whose intensity increases gradually with temperature. As previously described,[21] these peaks are assigned to the apical and basal P atoms of molecular P_4Se_3 formed at elevated temperature due to a depolymerization process affecting the melt.

Somewhat unusual behavior is seen for the melt containing 48 atom % P (Figure 3f), which is easily understood, however, with reference to its DSC thermogram (Figure 4). Heating this glass above T_g initially causes the ^{31}P NMR spectrum to broaden significantly, due to recrystallization under formation of crystalline P_4Se_4. This compound subsequently melts incongruently above 300 °C resulting in a substantially increased concentration of molecular P_4Se_3 in the melt. Upon cooling, the phosphorus speciation responds with pronounced hysteresis: the majority of P_4Se_3 units remain in the molten state, while the formation of crystalline P_4Se_4 (or an analogous amorphous species) appears retarded (spectra not shown).

Finally, at temperatures above 400 °C the spectra of glasses with P contents ≥40 atom % show the manifestations of chemical exchange between molecular P_4Se_3 and the remaining P atoms in the melt. The kinetic analysis of this process has been described previously in detail[21] and will not be discussed here.

Discussion

^{31}P Chemical Shifts in the Fast-Exchange Limit. Figure 5a summarizes the temperature dependence of the ^{31}P chemical shifts beyond the point of coalescence for all of the melts studied. In analogy with the interpretation of the ^{77}Se NMR spectra, the chemical shifts in this regime correspond to the weighted averages of the chemical shifts of each species involved in the exchange. Specifically, three distinct phosphorus sites, namely $Se{=}PSe_{3/2}$ groups, $PSe_{3/2}$ groups, and P—P bonded structures, must be

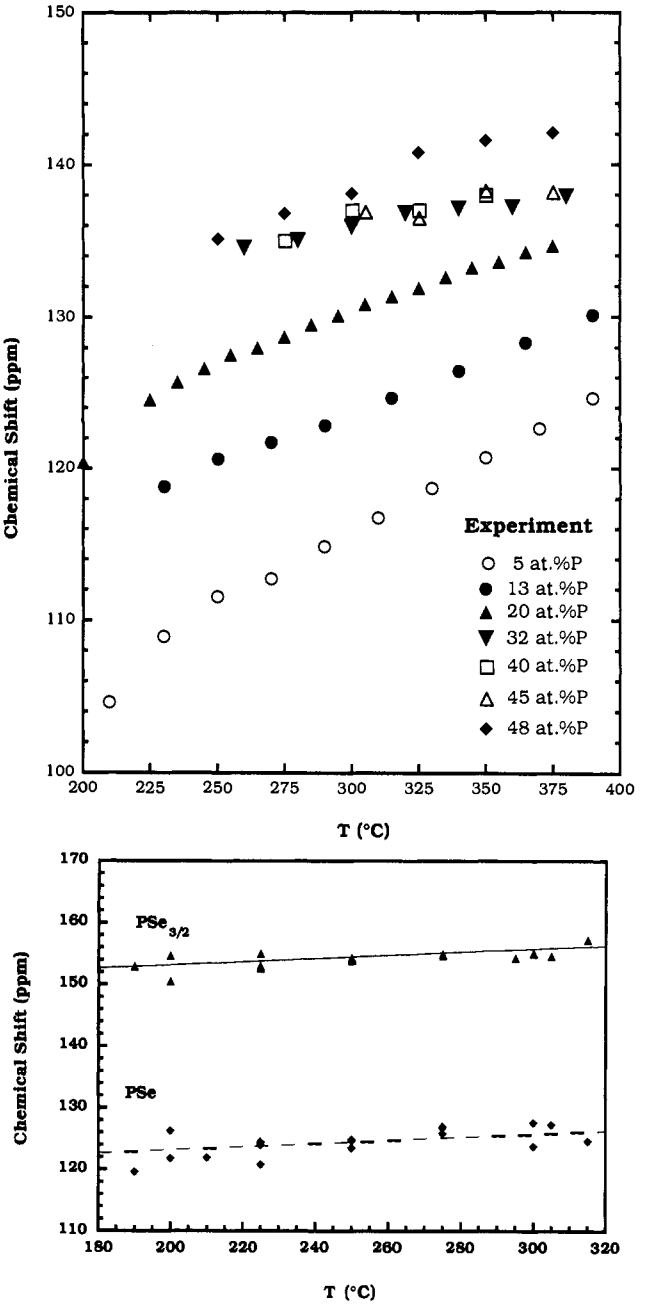

Figure 5. (a, Top) Temperature dependence of the ^{31}P chemical shifts in the fast-exchange limit. (b, Bottom) ^{31}P chemical shifts as a function of temperature for resolved resonances belonging to $PSe_{3/2}$ and PSe groups, respectively. Included are data for all glasses with P contents ≥28 atom %. The solid lines are defined by eqs 2a and 2b.

considered. While a variety of different types of P—P bonded structures are possible, we will assume for simplicity that all of them assume the form of $Se_{2/2}P{-}PSe_{2/2}$ groups. Phosphorus atoms present in this form will in the following be denoted in terms of "PSe units", expressing the correct P/Se ratio, albeit not the correct bonding geometry.

Quantitative estimates of these phosphorus structural units have been given previously based on spin–echo and MAS NMR.[18] Figure 5b summarizes chemical shift data measured for resolved resonances for $PSe_{3/2}$ and PSe groups in the temperature regime where the spectra have the multipeak appearance mentioned above. Data are included for various melts with phosphorus concentrations ≥28 atom %. Most notably, this figure illustrates that the specific chemical shift vs temperature curves for these units are approximately independent of melt composition. Linear least-squares fitting yields:

Table 2. Species Concentrations in PSe Glasses from Reference 18[a]

sample	*a*	*b*	*c*
5 atom % P	0.029	0.000	0.022
13 atom % P	0.084	0.000	0.041
20 atom % P	0.138	0.010	0.052
32 atom % P	0.180	0.100	0.042
40 atom % P	0.132	0.248	0.020
45 atom % P	0.104	0.342	0.005
48 atom % P	0.100	0.380	0.000

[a] *a*, *b*, and *c* represent the concentrations of the $PSe_{3/2}$, $Se_{2/2}P—PSe_{2/2}$, and $Se{=}PSe_{3/2}$ units, respectively.

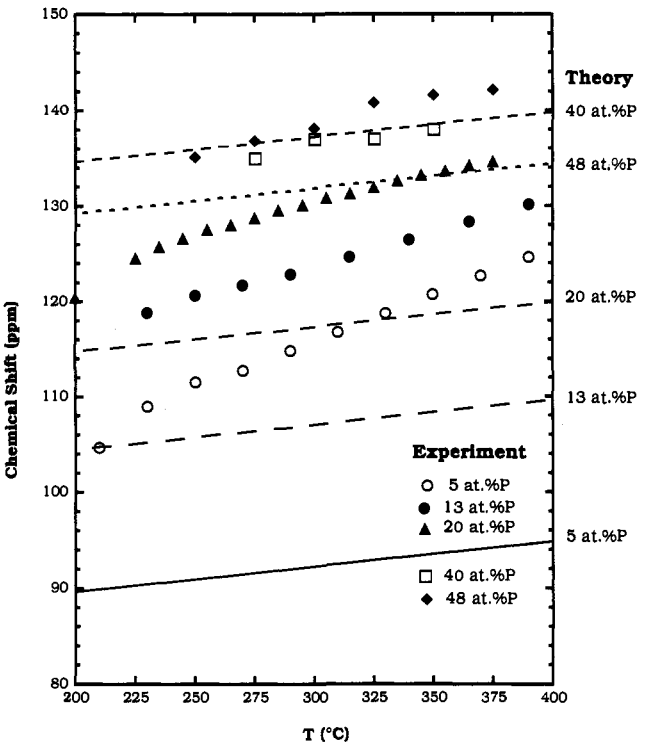

Figure 6. Comparison of actual and predicted (see text) ^{31}P chemical shifts in the fast-exchange limit in selected P–Se glasses.

$$\delta(PSe_{3/2}) = 148 \text{ ppm} + 0.026T\,(°C) \quad (2a)$$

$$\delta(PSe) = 118 \text{ ppm} + 0.026T(°C) \quad (2b)$$

The ^{31}P chemical shift temperature coefficient of 0.026 ppm/K is also observed for the model compound P_4Se_3 in the molten state and appears to be an intrinsic property of this system in the absence of chemical change. Assuming the same intrinsic temperature dependence for the $Se{=}PSe_{3/2}$ groups, we further approximate:

$$\delta(Se{=}PSe_{3/2}) = 0 \text{ ppm} + 0.026T\,(°C) \quad (2c)$$

In the fast-exchange limit an average chemical shift is measured:

$$\delta_{ave} = [a\delta(PSe_{3/2}) + b\delta(PSe) + c\delta(Se{=}PSe_{3/2})]/(a + b + c) \quad (3)$$

where *a*, *b*, and *c* correspond to the mole fractions of the respective species involved, and $a + b + c = \{P\}$, the total mole fraction of phosphorus. Using estimates previously published (Table 2),[18] and eqs 2a–c we can predict the corresponding ^{31}P chemical shift curves as a function of composition, in the absence of any chemical change. Figure 6 compares this prediction with the actual experimental data for selected glasses. Note the good agreement between experiment and prediction for the glass containing 40 atom % P. For other glasses, however, this comparison reveals significant discrepancies:

(a) In the low-phosphorus region (≤32 atom % P) the slopes of the chemical shift vs temperature curves are not composition independent but increase strongly with decreasing phosphorus concentration. As discussed below, this behavior reflects the temperature dependence of the equilibrium $PSe_{3/2} + Se \leftrightarrow Se{=}PSe_{3/2}$.

Table 3. Speciation and Equilibrium Constants for the Equilibrium between $PSe_{3/2}$ (*a*) and $Se{=}PSe_{3/2}$ (*c*) Units As Discussed in the Text

T (°C)	*c*	*a*	K_1
	5 atom % P		
230	0.305	0.695	0.509
250	0.291	0.709	0.476
270	0.286	0.714	0.465
290	0.275	0.725	0.441
310	0.266	0.734	0.420
330	0.256	0.744	0.399
350	0.246	0.754	0.378
370	0.237	0.763	0.359
390	0.227	0.773	0.339
410	0.215	0.785	0.316
430	0.205	0.795	0.299
450	0.191	0.809	0.273
470	0.174	0.826	0.243
490	0.155	0.845	0.212
510	0.122	0.878	0.160
	13 atom % P		
230	0.238	0.762	0.484
250	0.229	0.771	0.460
270	0.225	0.775	0.450
290	0.221	0.779	0.440
315	0.213	0.787	0.419
340	0.206	0.794	0.399
365	0.197	0.803	0.378
390	0.189	0.811	0.360
425	0.175	0.825	0.324
475	0.146	0.854	0.261
	20 atom % P		
235	0.192	0.808	0.516
245	0.188	0.812	0.499
255	0.183	0.817	0.484
265	0.182	0.818	0.479
275	0.179	0.821	0.469
285	0.175	0.825	0.456
295	0.173	0.827	0.449
305	0.170	0.830	0.439
315	0.168	0.832	0.434
325	0.166	0.834	0.426
335	0.163	0.837	0.416
345	0.161	0.839	0.409
355	0.160	0.840	0.406
365	0.157	0.843	0.399
375	0.156	0.844	0.395
385	0.153	0.847	0.386
395	0.152	0.848	0.381
415	0.147	0.853	0.367
425	0.144	0.856	0.358
450	0.136	0.864	0.332
465	0.134	0.866	0.326
480	0.117	0.883	0.277
495	0.109	0.891	0.257
510	0.100	0.900	0.233

(b) The chemical shift for the polymeric phosphorus units in the sample containing 48 atom % P strongly deviates from expectation, with respect to both absolute values and temperature coefficients. This behavior is directly linked to the appearance and growth of the P_4Se_3 peaks and to the disappearance of the broad P_4Se_4 resonance. As discussed below, these features suggest an equilibrium of the form

$$6PSe \leftrightarrow P_4Se_3 + 2PSe_{3/2}$$

The Equilibrium $PSe_{3/2} + Se \leftrightarrow Se{=}PSe_{3/2}$. We have previously suggested that the chemical speciation of the phosphorus atoms in P–Se glasses with low P contents (≤32 atom % P) as observed by room-temperature MAS-NMR can be explained

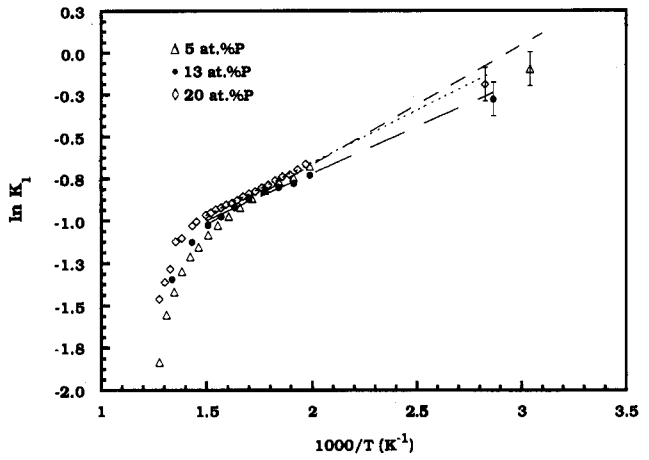

Figure 7. Temperature dependence of the equilibrium constant for the reaction $PSe_{3/2} + Se \Leftrightarrow Se{=}PSe_{3/2}$. The data shown at the respective T_g values originate from previous MAS-NMR experiments (ref 16).

in terms of a melt-equilibrium reaction:

$$PSe_{3/2} + Se \Leftrightarrow Se{=}PSe_{3/2}$$

The MAS-NMR spectra of P–Se glasses reflect the position of this equilibrium at the glass-transition temperature with the equilibrium constant

$$K_1 = [Se{=}PSe_{3/2}]/[Se][PSe_{3/2}] = 0.83 \qquad (4)$$

Previous results on P–Se thin films have suggested that these four coordinate species may be thermally unstable and break down at higher temperatures.[23] The variable-temperature NMR data reported above allow us to characterize this equilibrium in more quantitative detail. In this connection, the temperature coefficients of the chemical shifts and their distinct dependence on composition are of interest. The slopes in excess of the normal temperature dependence of 0.026 ppm/K essentially reflect a decrease in K_1 with increasing temperature. Evidently, the steepest chemical shift temperature dependences are observed at the lowest P content, because the fraction of $Se{=}PSe_{3/2}$ units is maximized there.

For glasses containing 20 atom % P or less, the mole fraction b of P-bonded phosphorus atoms can be neglected. Using the lever rule in conjunction with eq 3 thus simplified we obtain for fractions a and c:

$$c = \{P\}[(\delta_{av} - \delta_3)/(\delta_4 - \delta_3)] \qquad (5a)$$

$$a = \{P\}[1 - (\delta_{av} - \delta_3)/(\delta_4 - \delta_3)] \qquad (5b)$$

Here δ_4 and δ_3 are the chemical shifts of the $Se{=}PSe_{3/2}$ and $PSe_{3/2}$ groups, respectively, given by eqs 2a,b and {P} is the mole fraction of phosphorus in the glass. The concentration of free, i.e. non-phosphorus bound, selenium is given by

$$[Se] = \{Se\} - 1.5a - 2.5c \qquad (5c)$$

where {Se} is the total mole fraction of selenium in the glass. Thus, K_1 can be written as a function of just the exchange averaged chemical shift and the chemical shifts of the reference points δ_3 and δ_4, given by eqs 2a–c. Table 3 shows the results of this analysis for the low-P-content glasses. Listed are the concentrations of each species and the equilibrium constant for each temperature for the low-P-content glasses.

Van't Hoff plots, shown in Figure 7, clearly show wide linear segments in the temperature dependence of the equilibrium constant. Extrapolation of these curves in the low-temperature regime to the respective glass transition temperatures yields K_1 = 1.05, 0.79, and 0.87 (atom fraction)$^{-1}$ for the glasses containing 5, 13, and 20 atom % P. These values are in excellent agreement with the corresponding values of 0.91, 0.76, and 0.83 (atom fraction)$^{-1}$ determined previously by MAS-NMR for these three samples.[18] Table 4 summarizes enthalpies and entropies for the reaction $PSe_{3/2} + Se \Leftrightarrow Se{=}PSe_{3/2}$ extracted from the low-temperature curves in Figure 7. The reaction enthalpy around −5 kJ/mol indicates that the $Se{=}PSe_{3/2}$ groups form in an exothermic reaction; however, the reaction entropy is negative as expected. Thus, the thermal decomposition of the $Se{=}PSe_{3/2}$ groups is driven by the gain in entropy. Lastly, Figure 7 suggests that $\Delta_R H$ (as obtained from the slope) increases with increasing temperature. If we expand $\Delta_R H(T) = \Delta_R H(T_g) + \Delta_R c_p(T - T_g)$, we find that this change is consistent with a negative $\Delta_R c_p$ as expected for this reaction. We cannot rule out, however, that this temperature dependence of $\Delta_R H$ reflects the additional influence of yet another mechanism, such as the rupture of Se–Se bonds.

(23) Kumar, A.; Malhotra, L. K.; Chopra, K. L. *J. Noncryst. Solids* **1989**, *107*, 212.

Table 4. Reaction Enthalpies Derived from Chemical Shift Analysis of Equilibrium Involving $PSe_{3/2}$ and $Se{=}PSe_{3/2}$ Units As Described in the Text

sample	ΔH_R (kJ/mol)	ΔS_R (J/(mol K))
5 atom % P	−5.9 ± 0.3	−17.3 ± 0.6
13 atom % P	−4.6 ± 0.4	−15.2 ± 0.7
20 atom % P	−5.2 ± 0.1	−15.8 ± 0.1

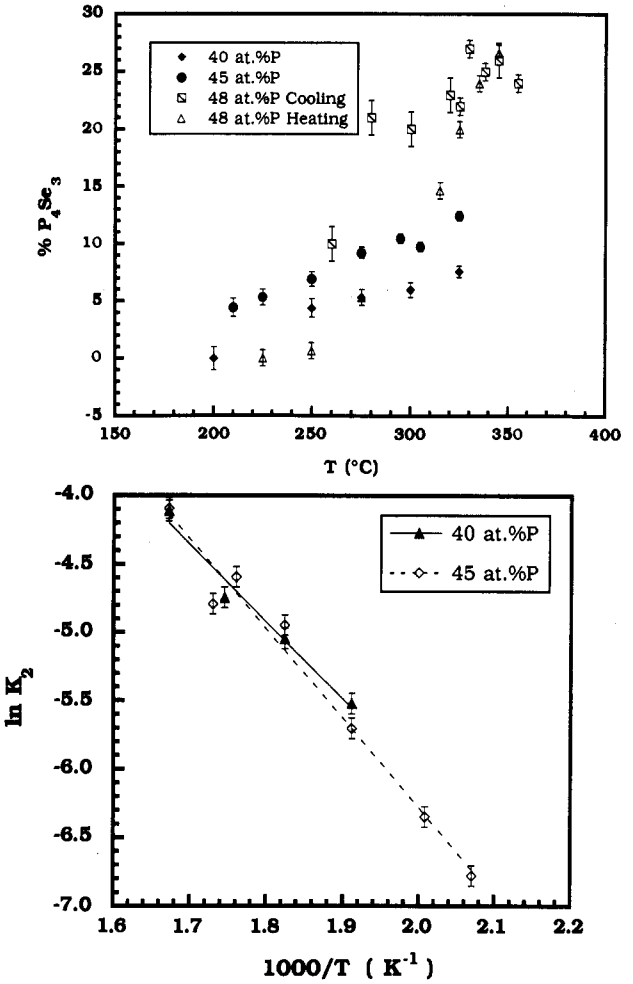

Figure 8. (a, Top) Percentages of P atoms present in the form of molecular P_4Se_3 in melts containing 40, 45, and 48 atom % P. (b, Bottom) Temperature dependence of the equilibrium constant for the reaction $3PSe \Leftrightarrow 2PSe_{0.75} + PSe_{3/2}$.

The Equilibrium $6PSe \Leftrightarrow P_4Se_3 + 2PSe_{3/2}$. Figure 8a depicts the percentages of P atoms present in the form of molecular P_4Se_3 for the melts containing 40, 45, and 48 atom % P (heating and cooling curve for the latter). As previously discussed, the

temperature-dependent creation of molecular P_4Se_3 proceeds via two distinct mechanisms: the process operative in the heating curve of the melt containing 48 atom % phosphorus is incongruent melting of a crystallized phase P_4Se_4, which formed due to annealing above T_g. The process operative in the melts containing 40 and 45 atom % P, which do not recrystallize, and in the cooling curve of the 48 atom % P glass is probably an analogous re-equilibration of the microstructural species in the molten state. In a previous publication, we developed a rather generic phenomenological description of this process, with no specific assumptions made about the types of species involved. In contrast, the results obtained in the present study allow us to postulate and discuss specific depolymerization processes. Two reasonable possibilities are the following reactions:

$$4PSe(P_4Se_4) \Leftrightarrow P_4Se_3 + Se \quad (6)$$

$$6PSe(1.5P_4Se_4) \Leftrightarrow P_4Se_3 + 2PSe_{3/2} \quad (7)$$

If process 6 were dominant, the ^{77}Se NMR data should reveal formation of free selenium, which is, however, not observed. In contrast, process 7 leads to the formation of $PSe_{3/2}$ groups and should thus result in an unusually strong temperature dependence of the ^{31}P chemical shift, as the balance of structural units in the melt shifts from the PSe species to the $PSe_{3/2}$ groups, which resonate significantly farther downfield. Figure 5 illustrates that this phenomenon is indeed observed in the 45 atom % and particularly the 48 atom % P melt, thus lending credence to the proposed reaction 7. If we rewrite eq 7 in the form

$$3PSe \Leftrightarrow 2PSe_{0.75} + PSe_{3/2} \quad (7a)$$

the equilibrium constant for this reaction is given by

$$K_2 = [PSe_{0.75}]^2[PSe_{3/2}]/[PSe]^3 \quad (8)$$

Denoting $[PSe_{0.75}]$ at equilibrium by the symbol d, we obtain

$$[PSe_{3/2}] = a + d/2 \text{ and } [PSe] = b - 3d/2$$

where a and b are the respective phosphorus fractions previously determined by NMR on the glassy state,[18] and d is obtained from the integration of the P_4Se_3 peaks, shown in Figure 8a. Thus, we obtain

$$K_2 = d^2(a + d/2)/(b - 3d/2)^3 \quad (8a)$$

Table 5 summarizes K_2 values thus obtained for the glasses containing 40 and 45 atom % P as a function of temperature. Corresponding van't Hoff plots are shown in Figure 8b, which characterize reaction 7 by a reaction enthalpy around +51 kJ/mol and a reaction entropy of +50 J/(mol K) (see Table 6). Thus, the depolymerization is strongly endothermic but results in entropy gain due to the formation of molecular P_4Se_3. The extent to which the depolymerization occurs is driven by the gain in entropy. It is perhaps significant, that the above depolymerization process is only observed at P–Se glass compositions close to and above 40 atom % phosphorus. This composition, at which the average coordination number of phosphorus is 2.4, corresponds to the rigidity percolation threshold. Evidently, it is only near and above this threshold that the gain in entropy is sufficiently large to allow the highly endothermic depolymerization reaction to proceed to some extent.

Table 5. Speciation and Resulting Equilibrium Constants for the Depolymerization Process Described in the Text

T (°C)	$d[P_4Se_3]$	$[PSe_{3/2}]$	$[Se_{2/2}P—PSe_{2/2}]$	K_2 ($\times 10^3$)
		40 atom % P Glass		
250	0.018	0.141	0.222	4.008
275	0.021	0.143	0.216	6.443
300	0.024	0.144	0.212	8.705
325	0.030	0.147	0.202	16.41
		45 atom % P Glass		
210	0.018	0.113	0.315	1.130
225	0.021	0.115	0.310	1.752
250	0.028	0.118	0.300	3.344
275	0.037	0.122	0.287	7.120
295	0.042	0.125	0.279	10.12
305	0.039	0.124	0.283	8.309
325	0.050	0.129	0.267	16.70

Table 6. Reaction Enthalpies and Entropies for the Depolymerization Process Described in the Text

sample	ΔH_R (kJ/mol)	ΔS_R (J/(mol K))
40 atom % P	46.9 ± 5.4	43.6 ± 9.6
45 atom % P	54.5 ± 3.6	56.7 ± 6.9

Conclusions

We have shown that detailed structural and thermodynamic information about glass-forming systems can be obtained from the composition and temperature-dependent analysis of chemical shifts in the fast-exchange limit of the molten state. For the phosphorus–selenium system under investigation, the data generated in the present study not only are nicely consistent with the structural speciations previously derived from solid-state NMR but also provide unique insights into the thermodynamic factors responsible for these speciations. One further aspect intimately linked with glass formation, yet not discussed within the present study, is the molten-state kinetics in the intermediate temperature regime between T_g and the fast-exchange limit. Key to a better understanding of the dynamics of these systems is a detailed analysis of the complex ^{31}P and ^{77}Se NMR spectra observed in this temperature region. Results of such studies will be published shortly.

Acknowledgment. Financial support by NSF Grant No. DMR 92-21197 and by the UCSB Academic Senate is gratefully acknowledged. We also thank the Shell Development Company for donation of a 200-MHz NMR spectrometer. Finally, we are grateful for the assistance and experimental contributions of Ms. Carri Lyda and Mssrs. Hans Erickson, Thomas Tepe, and Jason Leone.